The paper was presented at the Eighth Meeting
"New Trends in Fatigue and Fracture" (NT2F8)
Ankaran, Slovenia, 23–24 October, 2008

Miodrag Kirić[1], Aleksandar Sedmak[1], Jasmina Lozanović[1], Radoljub Tomić[2]

A COMPARATIVE ANALYSIS OF ENGINEERING METHODS IN FRACTURE MECHANICS

UPOREDNA ANALIZA INŽENJERSKIH METODA U MEHANICI LOMA

Originalni naučni rad / Original scientific paper
UDK /UDC: 539.42
Rad primljen / Paper received: 30.11.2008.

Adresa autora / Author's address:
[1)] Innovation Centre, Faculty of Mechanical Engineering, University of Belgrade, asedmak@mas.bg.ac.rs
[2)] „Prva petoletka - NIC" AD

Keywords
- line spring model
- crack
- fracture
- conservatism
- elastic-plastic region

Ključne reči
- model opruga u nizu
- prslina
- lom
- konzervativnost
- elastično-plastična oblast

Abstract

In this paper King's line spring model for surface cracks is analyzed and it is shown that interesting relations can be derived starting from analytical expressions of the model. King's model is compared with the line spring model of Rice and Levi. Significant similarities between two models are shown, but King's model extends the application of the approach to elastic-plastic region. FAD based on EPRI approach and SINTAP method are also analyzed.

Izvod

U ovom radu je analiziran Kingov model opruga u nizu za površinske prsline i pokazano je da se, polazeći od analitičkih izraza datih u modelu, mogu izvesti interesantne zavisnosti. Kingov model je upoređen sa modelom opruga u nizu Rajsa i Livia. Pokazane su značajne sličnosti ovih modela, ali Kingov model proširuje primenu pristupa na elastično-plastičnu oblast. Analizirani su i FAD zasnovan na EPRI pristupu, kao i SINTAP method.

INTRODUCTION

Significance of surface cracks, frequently present in structural components, can be evaluated by fracture toughness if stress state and materialal data are known. Generally, exact solution of the problem is not avialable and experimental, numerical and approximate analytical methods of fracture mechanics are applied.

Fracture toughness is usually presented by the stress intensity factor (SIF) for given flawed component assuming tension and/or bending load and small scale yielding. As a measure of stress magnitude at the crak tip, SIF in linear elastic fracture mechanics (LEFM) is dependent on crack and component geometry. Fracture toughness can be also expressed by J integral, path independent, given in unit of force per unit of length. Being path independent, J integral value is affected by crack and component geometry. Critical J value at the initiation of stable ductile crack growth, J_{Ic}, is a measure of plane strain fracture toughness.

Experimental investigation of single-edge-notched bend (SEN-B) specimens has revealed some typical dependences of J integral on strain and crack size. In the elastic region J integral is the parabolic function of strain and beyond it is a linear function. The slope of the linear parts of J vs. strain curve depends on crack size. In contrast to bending, the slope for a large crack in tension is weakly dependent on crack size /1/. Corresponding value of applied J integral is large because applied strain is transmitted in full through material and is added to the strain field ahead of crack. This behaviour is described as net section yield, /2/. For very short crack (up to 1 mm) displacements imposed at specimen ends in testing contribute only slightly to the strain field ahead of crack, because they are absorbed as plastic strain along specimen length, thus producing small applied J values. This behaviour is described as gross section yielding. The crack is considered here as long if its length/depth ratio is ten or more, and for short crack this ratio is below five.

One of the most useful engineering methods is by no doubt the continuous line spring, or the line spring model (LSM). Established in /3/, it has been applied for plates and shells with success. The LSM basic concept, attributed to Irwin, is that the uncracked portion of the ligament is replaced with a through-crack of equal length as the surface

crack with unknown membrane forces and bending moments acting on through-crack surfaces. The LSM version simplified by King, /4/, has been applied in the analysis of surface cracks in large spherical storage tank weldments and pipelines for fitness-for-service assessment, /5, 6/, and was compared with experimental results, /4, 6-8/. The conservatism of SIF applied by King's model for short cracks of moderate depth in plates was investigated here by comparing calculated SIF values with detailed three-dimensional finite element solutions of Raju and Newman. Linear dependence of J integral on crack opening displacement (COD) is experimentally shown, /9/, in accordance with, also experimentally, linear dependence of COD on remote stress, /1/, and remote strain, /10/, in an extended elastic plastic region. Linear relations between J integral and crack tip opening displacement (CTOD) are also derived here by applying King's model.

THE LINE SPRING MODELS

The line spring model is an effective tool for evaluating SIF in the case of LEFM. In this way, the three-dimensional crack problem is made analytically tractable. The other approximation is the representation of component by a plate or a shell in order to suppress the coordinate in the thickness direction using plate or a shell theory.

The LSM model for part-through crack in a plate enabled approximate solutions for SIF by reducing the truly three-dimensional crack problem to an idealised two-dimensional problem for elastic material. The approximate solution along the central section of surface semi-elliptical crack appeared appropriate and convenient for practical use, /3, 4/.

The additional opening displacement and relative rotation introduced by an edge crack are related to tension, σ, and bending, m, stresses acting on the discontinuity through compliance. By using appropriate boundary conditions for tension and bending fields to relate additional displacement and rotation with σ and m, the LSM provides two integral equations for σ and m. The interesting feature of the model is that values of J and COD are calculated at the tip of the surface crack, because the calculation involves the question of the region of its applicability. In LSM regions near the end of the model through-crack, it corresponds to the plate free surface, where the LSM can become inapplicable.

The LSM can be applied to elastic-plastic region. This approach in most cases considers J integral that consists of an elastic and a plastic part, /4, 11/. This extension of LSM requires either the numerical solution of integral equations in incremental form, or modification of a finite element programme by line-spring analysis. Thus, widespread LSM application requires specialized computer codes. The interest in LSM lasted through decades because this model is simple for application, highly flexible in regards to the crack profile and can be extended to treat multiple crack problems of different geometries, /12/.

The Rice-Levy formulation of LSM

The LSM, introduced by Rice and Levy, is an attempt to solve the problem of tensile stretching and bending of a plate with surface crack partly penetrating through the thickness. The idea is to present part-through cracked section as a continuous spring, of both stretching and bending resistance with compliance coefficients chosen to match those of an edge cracked strip in plane strain, Fig. 1, /3/.

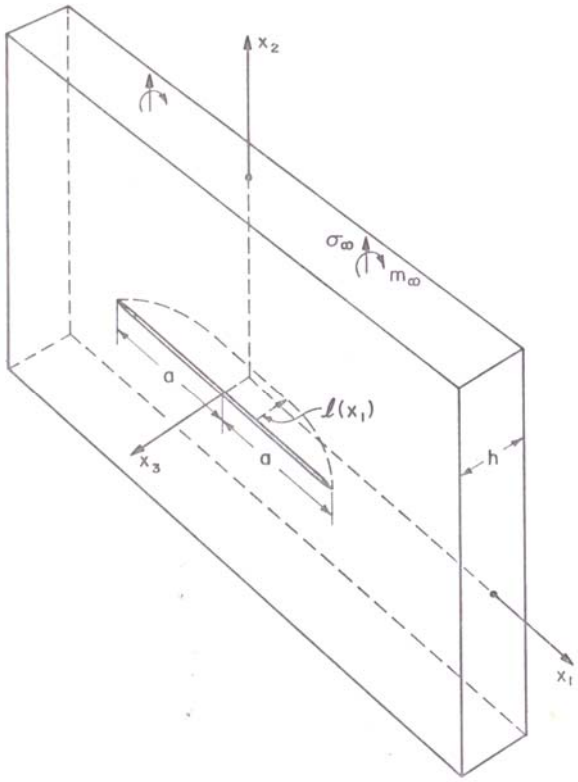

Figure 1. A surface crack partly penetrating plate thickness, /3/.
Slika 1. Površinska prslina koja prolazi kroz deo debljine ploče, /3/

The force and moment transmitted across the cracked section are computed calculating SIF at points along the crack tip. Simple approximate theories of generalized plane stress and Kirchoff-Poisson plate bending are employed together with a representation of the part-through surface crack as a continuously distributed line spring. For the two-dimensional problem of an infinite sheet in the x_1x_2 plane, average stress and nominal bending stress in the thickness are used, defined by integration over the sheet plate thickness in x_3 direction. Remote loads are denoted by σ_∞ and m_∞ in Fig. 1. For an edge crack in a plate loaded in tension and bending SIF is

$$K = h^{1/2}\left[\sigma g_t + m g_b\right] \tag{1}$$

where g_t and g_b are dimensionless functions of the crack depth l to thickness h ratio $\xi = l/h$. For $\xi < 0.7$ functions are

$$g_t = \xi^{1/2}\left(1.99 - 0.41\xi + 18.70\xi^2 - 38.48\xi^3 + 53.85\xi^4\right) \tag{2a}$$

$$g_b = \xi^{1/2}\left(1.99 - 2.47\xi + 12.97\xi^2 - 23.17\xi^3 + 24.80\xi^4\right) \tag{2b}$$

The additional displacement and rotation of one end of the strip relative to the other due to the introduction of the crack, δ and θ, respectively, are defined using compliance coefficients A_{ij}, where obviously $A_{bt} = A_{tb}$.

The generalized displacement h_δ, associated with σ and the generalized displacement $h_{2\theta}/6$, associated with m, are represented here by a column matrix of general displacements; also the compliance matrix **A** and column stress matrix are defined, related by Eq. (3)

$$\left\| \begin{matrix} h\delta \\ \dfrac{h^2\theta}{6} \end{matrix} \right\| = \left\| \begin{matrix} A_{tt} & A_{tb} \\ A_{bt} & A_{bb} \end{matrix} \right\| \left\| \begin{matrix} \sigma \\ m \end{matrix} \right\| \tag{3}$$

Irwin's relation between the potential energy release rate G and the rate of compliance change with crack length for the plane strain condition is generalized to the case of applied tension and bending loading:

$$G = \frac{1-\nu^2}{E} K^2 = h \frac{1-\nu^2}{E} (g_t^2\sigma^2 + 2g_t g_b \sigma m + g_b^2 m^2) \tag{4}$$

If, for example, only σ is applied and m is zero, one can obtain $h_\delta = A_{tt}\sigma$, and G is written as

$$G = \frac{1}{2}\sigma \frac{\partial}{\partial \ell}(h\delta) = \frac{1}{2}\sigma^2 \frac{dA_{tt}}{d\ell}, \quad m = 0 \tag{5}$$

The generalization for combined tension and bending is

$$G = \frac{1}{2}\left[\sigma \frac{\partial}{\partial l}(h\delta) + m \frac{\partial}{\partial l}\left(\frac{h^2\theta}{6} \right) \right] =$$

$$= \frac{1}{2}\left[\sigma \left(\frac{dA_{tt}}{dl}\sigma + \frac{dA_{tb}}{dl} m \right) + m \left(\frac{dA_{bt}}{dl}\sigma + \frac{dA_{bb}}{dl} m \right) \right] \tag{5a}$$

Unknown variables dA_{ij}/dl are calculated by equating common coefficients in quadratic forms of Eq. (5), using the symmetry for A_{tb}. After integrating, the expressions for δ and θ are given here by the matrix equation

$$\left\| \begin{matrix} \delta \\ \theta \end{matrix} \right\| = \frac{2(1-\nu^2)}{E} \left\| \begin{matrix} h\alpha_{tt} & h\alpha_{tb} \\ 6\alpha_{bt} & 6\alpha_{bb} \end{matrix} \right\| \left\| \begin{matrix} \sigma \\ m \end{matrix} \right\| \tag{6}$$

The column matrix on the left hand side of Eq. (6) is the matrix of additional displacement and rotation; it is given by the product of the matrix of dimensionless compliance coefficients and the column stress matrix, where $\alpha_{\lambda\mu}$ are dependent on $\xi = l/h$.

$$\alpha_{\lambda\mu} = \frac{1}{h}\int_0^l g_\lambda g_\mu dl, \quad \lambda, \mu = b, t \tag{7}$$

The results of calculations for coefficients g_t and g_b using Eqs. (2a) and (2b) are given in Fig. 2, and in Fig. 3 for dimensionless compliance coefficients $\alpha_{\lambda\mu}$, using Eqs. (7), (6a) and (6b), employed for the line spring, /3/. The SIF value calculated at the midpoint of semi-elliptical crack using numerical integration and piecewise linear interpolation functions, is taken as a conservative estimate of SIF. It is divided by the SIF of an edge crack in plane strain for the same remote tensile or bending load and of depth as at the centre point. Results for dimensionless K are given for nominal tensile stress σ_∞ ($m_\infty = 0$) and nominal bending load m_∞ ($\sigma_\infty = 0$). Only results for SIF under pure tensile loading at midpoint of a semi-elliptical crack where $l(0)/h = l_o/h$ are illustrated here. The results of the model are in close agreement with presumably more accurate calculation given in Table 1, see Ref. /3/.

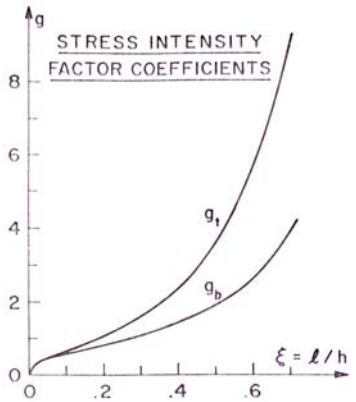

Figure 2. Coefficients g_t and g_b for an edge cracked strip.
Slika 2. Koeficijenti g_t i g_b za ivičnu prslinu

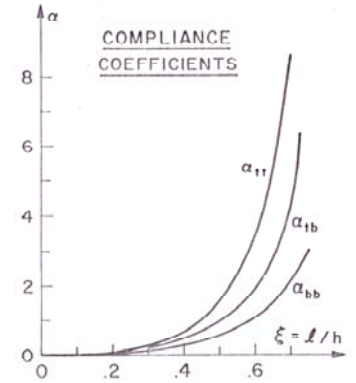

Figure 3. Compliance coefficients $\alpha_{\lambda\mu}$.
Slika 3. Koeficijenti popustljivosti $\alpha_{\lambda\mu}$

Table 1. Dimensionless K at semi-elliptical crack midpoint, $m = 0$.
Tabela 1. Bezdimenziono K na sredini polu-eliptične prsline, $m = 0$

l_o/h	$2a/h$	$K/(h^{1/2}\,\sigma_\infty)$	Reference result
0.1	0.25	0.41	0.42
0.2	0.4	0.48	0.51
0.2	0.5	0.52	0.60
0.3	0.6	0.57	0.63
0.3	0.75	0.63	0.73
0.4	0.8	0.68	0.70
0.4	1.0	0.76	0.84
0.5	1.0	0.82	0.82
0.5	1.25	0.90	0.94
0.6	1.2	0.96	0.91
0.6	1.5	1.06	1.15

Once σ and m are determined from integral equations, SIF at points along the crack tip is given by Eq. (1). The solution is given for a special case when each of the dimensionless compliance coefficients varies in the form

$$\alpha_{\lambda\mu}(X) = \alpha^{\circ}_{\lambda\mu}\sqrt{1 - X^2} \tag{8}$$

where $\alpha^{o}_{\lambda\mu} = \text{const}$, $X = x_1/a$ is a dimensionless coordinate and $\alpha^{o}_{\lambda\mu}$ is the value of $\alpha_{\lambda\mu}$ for $X = 0$. Integral equations are reduced to the system of equations which determine α and m:

$$\frac{1-\nu^2}{2}\frac{h}{a}\left[\alpha^{\circ}_{tt}\sigma + \alpha^{\circ}_{tb} m\right] + \sigma = \sigma_\infty \tag{9a}$$

$$\frac{3(3+\nu)(1-\nu)}{2}\frac{h}{a}\left[\alpha^{0}_{bt}\sigma + \alpha^{0}_{bb} m\right] + m = m_\infty \tag{9b}$$

It is claimed that the only shape of a crack which is consistent with the assumed functional form of Eq. (8) is the case of a very shallow crack, $l/h << 1$, of depth proportional to $(1 - X^2)^{1/4}$.

It is concluded also that the numerical solution of integral equations may be replaced by the simple approximation for σ and m, which gives a conservative overestimate to SIF.

King's model

The model introduces unknown force N per unit length and unknown moment M per unit length which act on crack faces; the average closure stress σ_c (instead of previous σ_∞) and nominal bending stress m (instead of previous m_∞), related by similar relations in both LSM models.

$$\sigma_c = N/h, \quad m = 6M/h^2 \tag{10}$$

It is assumed that load is carried partly by the edge crack and partly by the through crack between which displacement compatibility is enforced, Fig. 4, /4/.

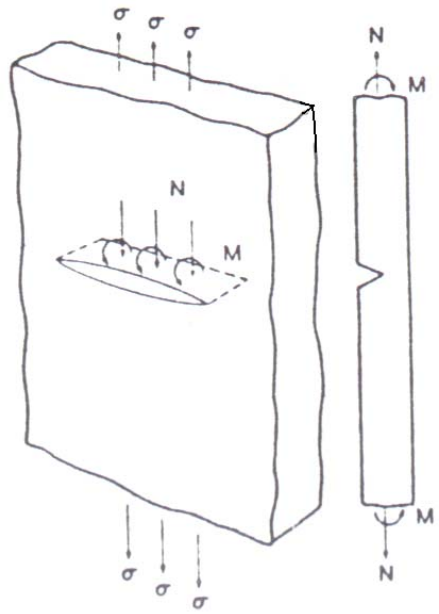

Figure 4. King's line spring model
Slika 4. Kingov model opruga u nizu

According to the critical COD model of Irwin, the remaining ligament yields and the surface crack behaves as a through-thickness crack of same length with the opening reduced by closure forces equal to the product of flow stress and the area of the uncracked ligament. The model gives the expression for COD in the middle of the central crack of length $2a$ in an infinite plate under a remote stress σ perpendicular to the crack plane. King's model assumes that COD is obtained for stress σ reduced by stress σ_c:

$$\text{COD} = 2l(\sigma - \sigma_c)/E \tag{11}$$

King's model uses Eqs. (6) as well as two additional simple expressions for displacement δ and rotation θ (being given, but not derived), in order to eliminate δ and θ from them. Thus obtained system of two equations in σ_c and m, Eqs. (7) and (8), /4/, that correspond to Eqs. (9) here, but given in a different form, are solved and solutions are written as

$$\sigma_c = \alpha\sigma, \quad m = -\beta\sigma \tag{12}$$

with α and β being functions of ratio l/h, dimensionless compliance coefficients $\alpha_{\lambda\mu}$ and Poisson's coefficient ν.

It can be shown that LSM model Rice-Levy contains the same equations as Eqs. (12) of King's model for the special case when Eq. (8) is fulfilled and if $m_\infty = 0$.

In the King's model the crack half-length a is extended by the plastic zone of diameter $2r_y$ ($a_p = a + 2r_y$), where a_p is given in implicit relation between plate width W, σ_c, σ and flow stress σ_F. The other feature of the King's model are the defined ligament yield stress, σ_{LY}, and net section yield stress, σ_{NSY}. The plate will carry the load up to strip yielding of the plate edge, what occurs when the applied stress is equal to σ_{NSY}. In this way the model gives expressions for J integral, CTOD and CMOD for linear elastic and elastic-plastic regions. Thus in the elastic-plastic region

$$J = J_{el} + J_p, \quad \sigma_{LY} < \sigma < \sigma_{NSY} \tag{13}$$

where the elastic part J_{el} is given by Eq. (4) for $\sigma = \sigma_{LY}$ and using Eq. (1) for an edge crack. The plastic part J_p reads:

$$J_p = \sigma_F(\delta - \delta_{LY}) \tag{14a}$$

with δ_{LY} calculated at $\sigma = \sigma_{LY}$, so that

$$J_p = \frac{4\sigma_F}{E}\left[(a + r_y)\sigma - a\sigma_{LY} - \left(1 - \frac{l}{h}\right)r_y\sigma_F\right] \tag{14b}$$

Similar expressions are obtained for CTOD and CMOD, derived under the assumption of small rotation angle θ.

The model is applicable to parameters for flat plates in tension. The remote stress is the nominal membrane stress normal to the crack plane, thus redistribution of stresses caused by the crack is neglected. This simplified model can be applied when the crack length is short in comparison to a dimension of the component. For circumferential flaws in pipes, the errors can be expected if curvature is neglected.

Typical comparison of model behaviour prediction with experimental data of measured CMOD and J integral in testing of tensile panel of steel API-5LX-70 containing surface cracks is shown in Fig. 5. Satisfactory agreement is shown and σ_{NSY} is accurately modelled because the tested steel had exhibited a small strain hardening coefficient, /4/.

Improvement of some features of King's model

The results of King's model will be analysed in order to establish relations between basic parameters (applied stress, J integral, CMOD and CTOD). The flat tensile panel, made of steel TSt.E460, of yield strength $\sigma_y = 470$ MPa, of width $W = 300$ mm and thickness 20 mm, with central crack of depth 9 mm and length 52 mm, is tested, /13/. The flow stress is $\sigma_F = 550$ MPa. Calculation is performed here with $\sigma_{LY} = 356.9$ MPa and $\sigma_{NSY} = 507$ MPa. Calculated J integral values are shown together with approximate polynomials of the fourth and the fifth order large stress value range, and of the second order polynomial for small stress value range, which fits almost perfectly, Fig. 6. Correlation coefficients R are given in parentheses. Approximation error is SD. The higher the polynomial order, the better the approximation. The fifth order polynomial is acceptable here, /14/.

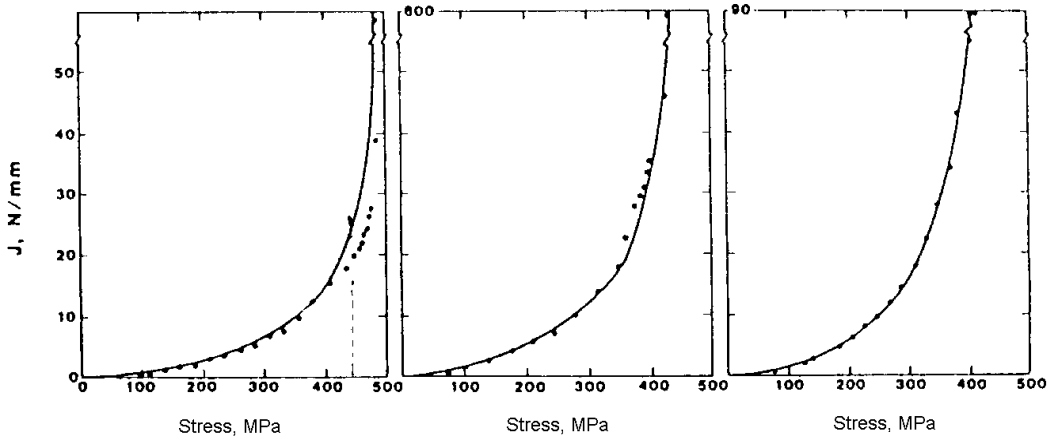

Figure 5. Comparison of model solutions and experiment, /4/.
Slika 5. Poređenje rešenja modela i eksperimenta, /4/

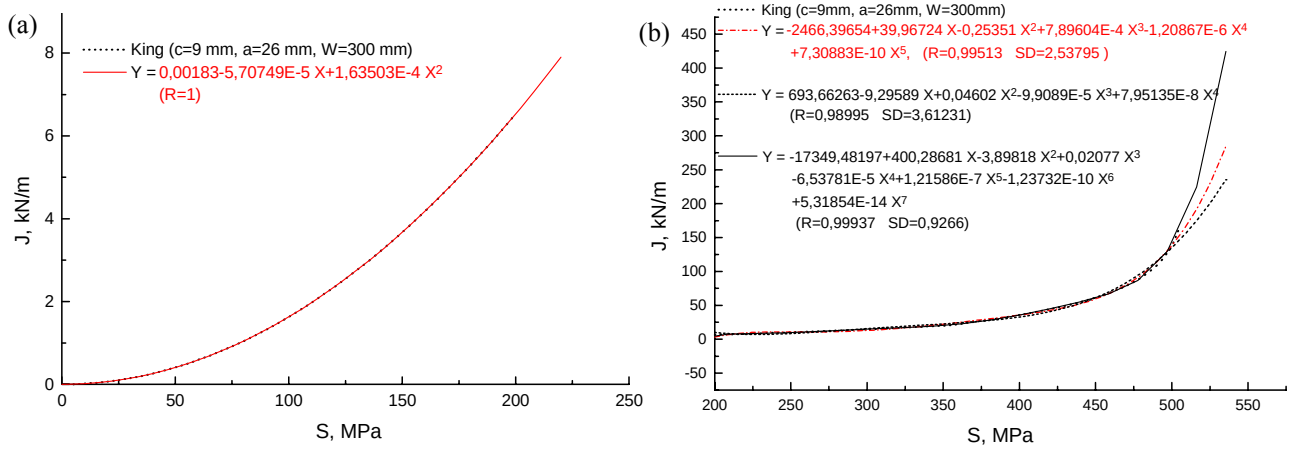

Figure 6. *J* integral versus applied stress *S* for linear-elastic (a) and in elastic-plastic region (b).
Slika 6. Zavisnost *J* integrala od primenjenog napona *S* za linearno-elastičnu (a) i elasto-plastičnu oblast (b)

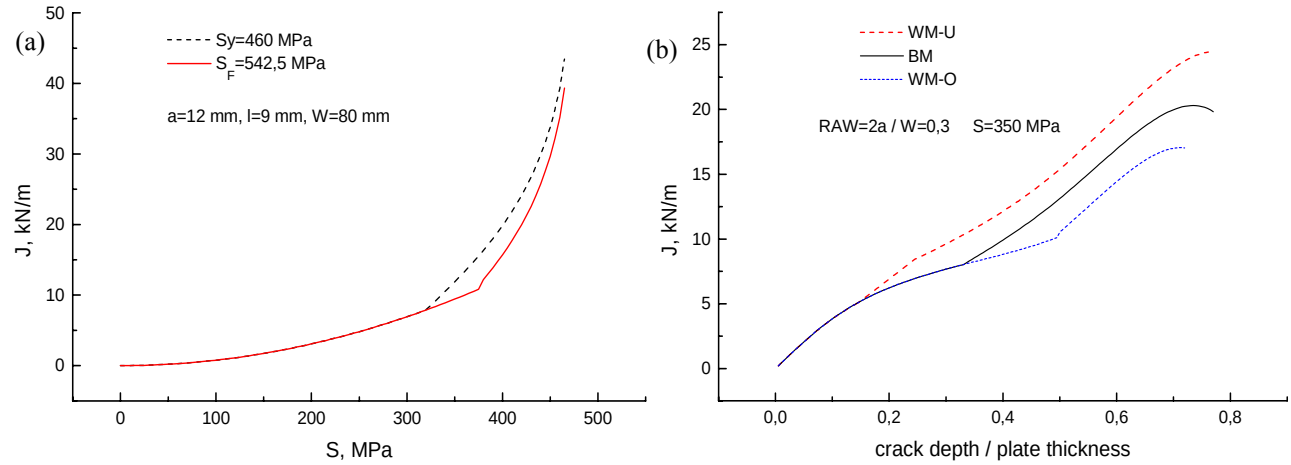

Figure 7. *J* integral versus applied stress *S* for linear-elastic (a) and elastic-plastic region (b).
Slika 7. Krive *J* integral–primenjen napon S u linearno-elastičnoj (a) i elasto-plastičnoj oblasti (b)

Tensile properties are taken for parent metal (BM), steel TSt.E460, $\sigma_y = 460$ MPa, $\sigma_F = 542.5$ MPa, for undermatched weld metal (WM-U), $\sigma_y = 400$ MPa, $\sigma_F = 500$ MPa, and for overmatched weld metal (WM-O), $\sigma_y = 520$ MPa, $\sigma_F = 585$ MPa, /10/. The central crack (depth $l = 9$ mm, length 24 mm) is made in BM or in WM, in the plate (width $W = 80$ mm, thickness $h = 20$ mm). Yield stress of the ligament was calculated by King's model, σ_{LY} with σ_F, but if σ_F is replaced by yield strength for uniaxial tension σ_y, Eq. (15), a little bit earlier and steeper increase of the *J* integral is obtained with remote stress opposed to when σ_{LY} is defined according to the model, Fig. 7a:

$$\sigma_{LY} = (1 - l/h)\alpha^{-1}\sigma_F \quad \rightarrow \quad \sigma_{LY} = (1 - l/h)\alpha^{-1}\sigma_y \quad (15)$$

where coefficient α is defined in the model, /4/.

In Fig. 7a, S_F denotes σ_F. Thus the conservatism of King's model can be increased. A resistance curve can be

used to compare material properties, (Fig. 7b): for the same crack, the crack driving force is higher in weaker material.

Similar results are obtained for J integral (Fig. 8a). Slopes of curves for WM in similar diagrams (Fig. 8) differ from the slope for BM: WM-O has the smallest, and WM-U the largest slope, thus J integral and CMOD of weaker WM are the largest for the same stress. The second case is inconvenient for weld joint integrity, since for the same crack driving force, CMOD is the largest for WM-U. Shielding effect of stronger WM-O is expressed in smaller CMOD for (large) crack, and plastic strains are in a region remote from the welded joint. The border between linear-elastic and elastic-plastic range for BM is about 300 MPa, thus the right side diagram mainly covers the elastic-plastic region. The relation between J and CTOD is analysed on the same specimen for remote stress (linear-elastic and elastic-plastic), Fig. 9. They are of linear regressions with regression coefficients greater than 0.998.

In this way King's model provides an analytical method for structural integrity assessment in elastic-plastic range.

The relation J vs. CTOD calculated in the elastic-plastic range for σ_y = 470 MPa, is theoretically linear, /15/. For the considered example (W = 300 mm), using King's model, diagrams given in Fig. 9 and linear regression in terms of σ_y in Eq. (16) are obtained. The Eq. (16) is in agreement with the expected relation for plane stress, /16, 17/.

Implementing the results from Eq. (15) for $2a$ = 52 mm, l = 9 mm, h = 20 mm, $\sigma \geq$ 200 MPa to Eq. (16), the relation J integral vs. CTOD is closer to theoretical value, Eq. (17):

$$J \approx 1.15\,\sigma_y\,\mathrm{CTOD} \qquad (16)$$

$$J \approx 1.02\,\sigma_y\,\mathrm{CTOD} \qquad (17)$$

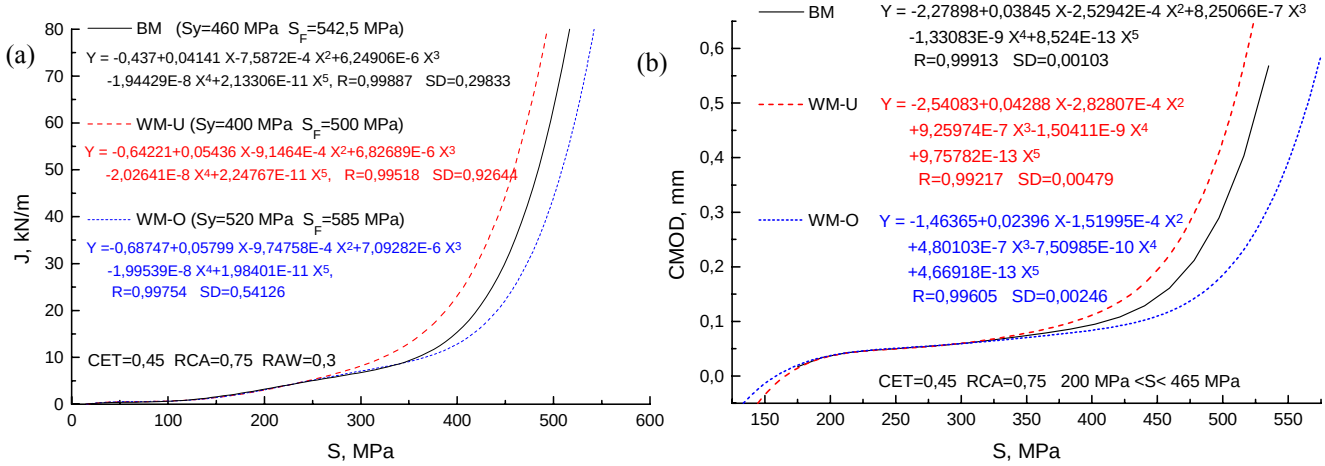

Figure 8. The influence of metal properties on J integral (a) and CMOD dependence (b) on remote stress in elastic-plastic region.
Slika 8. Uticaj osobina metala na zavisnost J integrala (a) i CMOD (b) od udaljenog napona u elasto-plastičnoj oblasti

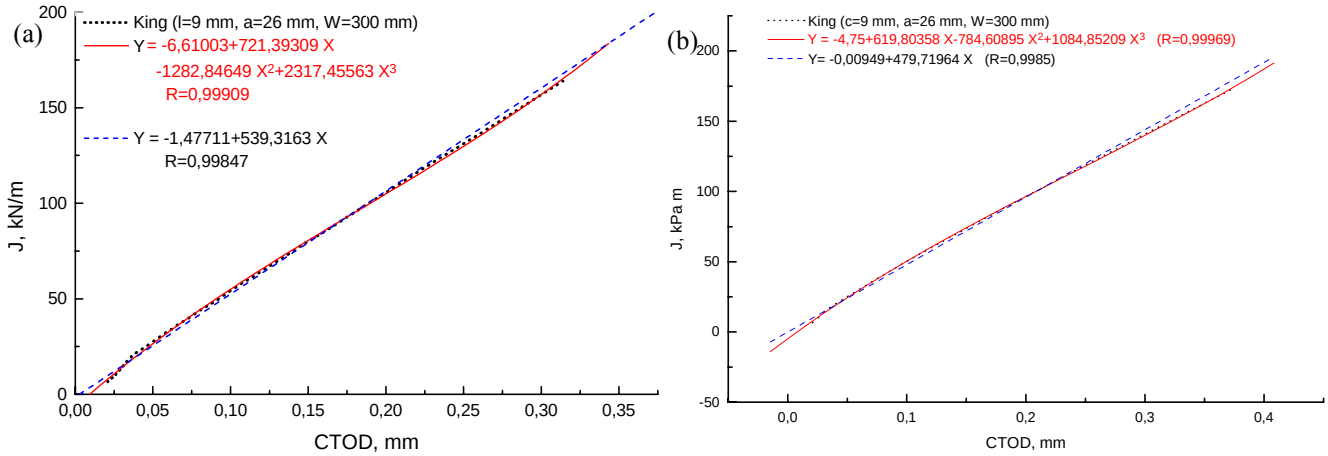

Figure 9. The linear relation between J integral and CTOD (King's model for σ_{LY} defined by σ_F = 550 MPa (a) and by σ_y = 470 MPa (b)).
Slika 9. Linearna zavisnost J integrala i CTOD (model Kinga za σ_{LY} određeno sa σ_F =550 MPa (a) i sa σ_y = 470 MPa (b))

FAILURE ASSESSMENT DIAGRAM

One-parameter approach of LEFM is not applicable to components with large scale yielding at the crack tip, when tensile stress is close to material yield strength. In order to include such real situations, generally between two limiting cases – the brittle fracture and plastic collapse, the two-parameter approach of fracture mechanics is applied, introducing the failure assessment diagram (FAD). The failure assessment curve (FAC), defined by the functional dependence of the relative stress intensity factor (SIF), K_r, on relative stress S_r, is the boundary line between unsafe region above it and safe region below it, where fracture is not expected, /18, 19/.

FAD and secondary stresses

The failure assessment procedures of the CEGB and SINTAP assume that secondary stresses do not influence

fracture when the structure fails by plastic collapse, thus they are not taken into account in determining S_r nor the limit load, or the degree of ligament plasticity L_r, but they are taken into account in determining K_r.

Total SIF value is obtained by superimposing contributions of primary and secondary stresses, K_I^p and K_I^s, respectively, around the crack tip /20, 21/.

$$K_r = \frac{K_I}{K_{Ic}} = \frac{K_I^p + K_I^s}{K_{Ic}} \tag{18}$$

In as-welded components and if the residual stress (RS) distribution is not known, an uniform distribution may be assumed and magnitude equal to the appropriate material yield strength σ_y for levels 1 and 2, /21/. In the analysis for level 2, applied in here, it can be taken as the lower of

$$\sigma_y \quad \text{or} \quad \left(1.4 - \frac{\sigma_n}{\overline{\sigma}}\right)\sigma_y \tag{19}$$

where σ_n is the effective net section stress and $\overline{\sigma}$ is the flow stress. When a structure is loaded by primary stresses, a part of RS is relieved by plastic strain. A simple model of this mechanical stress relief is to assume that the sum of the primary load and RS cannot exceed the flow stress. For yield magnitude of RS in the unloaded state, the PD 6493 permits the use of Eq. (19) to compute K_I^s.

When secondary stresses are present, PD 6493 introduces a correction term for assessment levels 2 and 3 to allow for plasticity interactions of primary and secondary stresses by introducing the plasticity correction factor ρ:

$$K_r = \frac{K_I}{K_{Ic}} + \rho \tag{20}$$

The level of RS remaining after the PWHT for the low alloy steel is about 30% of the room temperature WM yield strength when stresses are parallel to the weld, i.e. if the crack is transverse to the weld. Transverse weld flaws are normally located within the zone of tensile stress, whose width is greater than the weld width. Even for flaws whose tips are located in the zone of compressive stresses, the net effect of the stress distribution is to produce a positive SIF.

For the level 1 and 2 estimation, the parameter S_r is calculated as

$$S_r = \sigma_n / \overline{\sigma} \tag{21}$$

If the flow stress is above $1.2\sigma_y$, the value $\overline{\sigma} = 1.2\sigma_y$ is taken to calculate S_r. For a constant crack size S_r is proportional to the applied load and K_r given by Eq. (18) scales with load as a linear function, too. Thus, the points (S_r, K_r) for increasing load and the constant crack size can be displaced along the ray through the origin, as it is shown in references (20, 22). It means that the plasticity correction factor ρ in Eq. (20) is neglected, as it is done here, but in general the relation is not linear, as it is stated in Ref. /22/.

For a through-thickness crack the conservative estimate of applied SIF is calculated using the expression

$$K_I = \sigma_1 \sqrt{\pi a} \tag{22}$$

where σ_1 is the maximum value of tensile stress in cross section and $2a$ is the crack length.

The calculation of FAD

Tensile specimens sized 300×80×20 mm are welded by the submerged-arc welding (SAW). Cracks are made by electrical discharge machining, and of length $2a$ = 24 mm and 9 mm deep, with tips 0.1 mm wide, located in the heat affected zone (HAZ). The influence of PWHT on RS is estimated for the centre cracked specimen (MT panel) made of HSLA steel TStE 460, with known values σ_y = 460 MPa, $\overline{\sigma}$ = 542.5 MPa, ε_0 = 0.002, α = 1.12, /23/. The difference in yield strength of the parent metal (BM) and overmatching weld metal (WM-O) is not considered because the approach should be conservative. According to PD 6493 it is assumed that RS is equal to σ_y in the as-welded condition and that RS is equal to $0.3\sigma_y$ after the PWHT, the latter being a more conservative criterion than Eq. (19). The correction for finite specimen width is applied, /15, 20/

$$K_I = \sigma_1 \sqrt{\pi a}\left[\sec\left(\frac{\pi RaW}{2}\right)\right]^{1/2} \times$$
$$\times(1 - 0.025RaW^2 + 0.06RaW^4) \tag{23}$$

where RaW is the ratio of crack length $2a$ = 24 mm and specimen width W = 80 mm (RaW = 0.3).

An external force P is introduced, producing a remote membrane tensile stress σ^P in the specimen. Corresponding S_r^t values are calculated using the formula derived from Eq. (21) which takes into account the RaW ratio:

$$S_r^t = \frac{\sigma^P}{\overline{\sigma}(1 - RaW)} \tag{24}$$

The derivation of the equation defining the R-6 curve postulates small scale yielding (where RS have a significant influence on fracture), and thus is used in FAD based on J-controlled crack growth with the abscissa given by the ratio

$$S_r^{EPRI} = \frac{P}{P_0} \tag{25}$$

where P and P_0 are forces per unit thickness, and P_0 is the limit load for plain stress

$$P_0 = 4d\sigma_0 \big/ \sqrt{3} \tag{26}$$

and with K_r depending on J integral elastic solution, J_e, which is the function of the effective crack length a_e and P, as well on J integral as a function of stable crack extension, $J_R(\Delta a)$, /20, 24/

$$K_r = \sqrt{J_r} = \sqrt{J_e(a_e, P) \big/ J_R(\Delta a)} \tag{27}$$

FAD diagram calculated for a centre through-thickness crack using FORTRAN program and four values of P and two levels of RS is given in Fig. 10. Solid lines represent points for residual stress level equal to σ_y and corresponding to four P-values from 0.5 MN to 0.65 MN, with increment of 0.05 MN (first point is calculated for the lowest value – left hand side and the last point for maximal load value – right hand side. Corresponding linear regression, with correlation coefficient R = 0.99998, is given in Fig. 10, as well as FACs based on J-controlled crack growth for n = 5, 10 and 20.

Representative points for the state after PWHT with RS = $0.3\sigma_y$ are plotted for the same four values of P, so for P increasing, points lay on a straight from the left to the right hand side on the diagram. These points are labelled as open and define the linear regression with $R = 1$.

Upper linear regression, the dashed line, gives K_r for the crack without the PWHT. The critical P value, i.e. the cross section of the linear regression line with the R-6 curve, determines the value $P_1 = 530$ kN, while the plane stress EPRI boundary curve for $n = 10$ (assumed $n = 10$ as for the value of the steel), determines critical value $P_2 = 50$ kN. For the state after PWHT, the critical P value determined by the R-6 is equal to $P_3 = 586$ kN, and by EPRI $P_4 = 664$ kN. The effect of PWHT can be estimated from the difference found between R-6 ($P_3 - P_1 = 56$ kN), and for case $n = 10$, ($P_4 - P_2 = 114$ kN).

The boundary curve for $n = 10$ allows an increment in critical P value, in as-welded state $P_2 - P_1 = 20$ kN and after PWHT $P_4 - P_3 = 78$ kN. The points are in straight lines along the K_r axis for a length proportional to RS value.

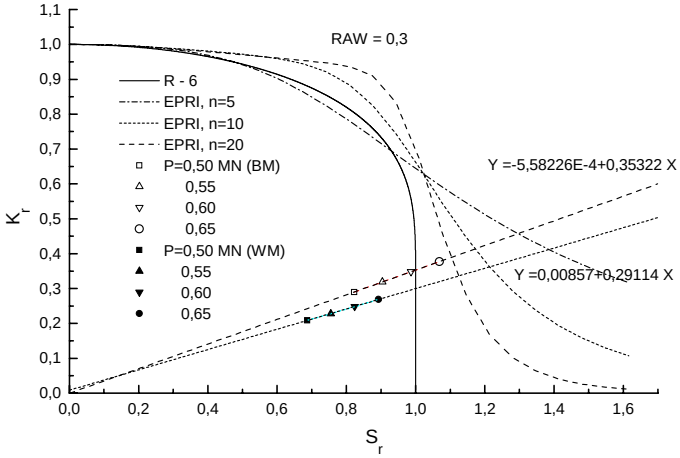

Figure 10. The effect of PWHT and tensile load P on the stability of through-thickness centre cracked specimen, $RaW = 0.3$.
Slika 10. Uticaj PWHT i zateznog opterećenja P na stabilnost uzorka sa centralnom prolaznom prslinom, $RaW = 0{,}3$

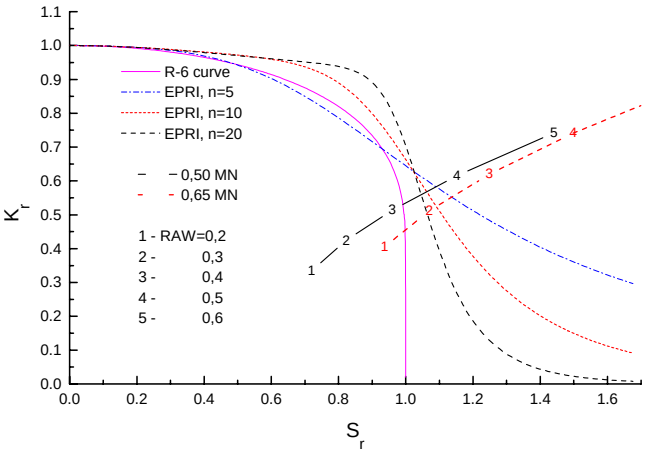

Figure 11. FAD analysis of tensile specimen containing the centre through-thickness crack of length $RaW = 0.3$.
Slika 11. FAD analiza zateznog uzorka sa centralnom prolaznom prslinom dužine $RaW = 0{,}3$

Failure analysis according to SINTAP

The values of the loading parameter L_r for the basic level of SINTAP are

$$L_r = \sigma_{ref}/\sigma_y = \sigma_n/\sigma_y \qquad (28)$$

and the values of the correction function $f(L_r)$

$$f(L_r) = \left(1 + \frac{1}{2}L_r^2\right)^{-1/2}\left[0.3 + 0.7\,\mathrm{e}^{-\mu L_r^6}\right], \quad 0 \le L_r \le 1 \qquad (29a)$$

$$f(L_r) = f(L_r = 1)L_r^{(N-1)/2}, \quad 0 \le L_r \le L_r^{max} \qquad (29b)$$

are calculated for the BM with parameters:

$$N = 0.3\left(1 - \sigma_y/R_m\right) \text{ and } L_{r\max} = \frac{1}{2}\frac{\sigma_y + R_m}{\sigma_y} \qquad (30)$$

For crack of length $2a = 24$ mm and ultimate tensile strength of the steel $R_m = 625$ MPa, values for $N = 0.0792$ and $L_{rmax} = 1.179$ are calculated. Results calculated for variable load are illustrated in Fig. 11 for as-welded condition (solid circles) with RS = σ_y and for the state after the PWHT (open circles) with RS = $0.3\sigma_y$. Points shown in the diagram correspond to six P values, of which the first is calculated for 0.5 MN and the last for 0.75 MN, going from left to right.

The critical P value for as-welded state is $P = 645$ kN and after the PWHT, $P = 695$ kN.

The influence of crack length and yield strength

Increase of crack constant load, S_r, depends linearly on crack area only if the crack area is small compared to the total cross section, since it is inverse to the effective net cross section. S_r and K_r are not proportional to the crack size at the same time, since K_I given by Eq. (22) or (23), is a nonlinear function of crack size. So, in general case, the failure path of increasing crack size is not a straight line, as it is sometimes illustrated, Ref. /19/, and is not the same as increasing load path for a crack of fixed length.

The relation between S_r^t and K_r^t is not linear, e.g. $K_r' = k(S_r' - S_r) + K_r$, where k is a constant.

The analysis is here illustrated in Fig. 12.

The diagram given left compares paths in FAD for given four tensile load values and for the same through-thickness crack in the same BM ($K_{Jc} = 220$ MPa·m$^{1/2}$ is an experimental value) and in the WM, overmatching the BM ($\bar{\sigma} = 650$ MPa). BM plastic collapse occurred at 600 kPa when using R-6 curve, while the specimen made of WM would be safe for all given P values.

The influence of load P when crack size RaW changes is analysed in the diagram on the right side in Fig. 12. It is seen that paths to failure for increasing RaW are not represented by straight lines.

Critical loads for three approaches are shown in Table 2.

Table 2. Critical loads obtained using different FACs (in kN).
Tabela 2. Kritična opterećenja dobijena za različite FAC krive (kN)

State	R-6	EPRI, $n = 10$	SINTAP
As welded	530	550	645
After PWHT	586	664	695

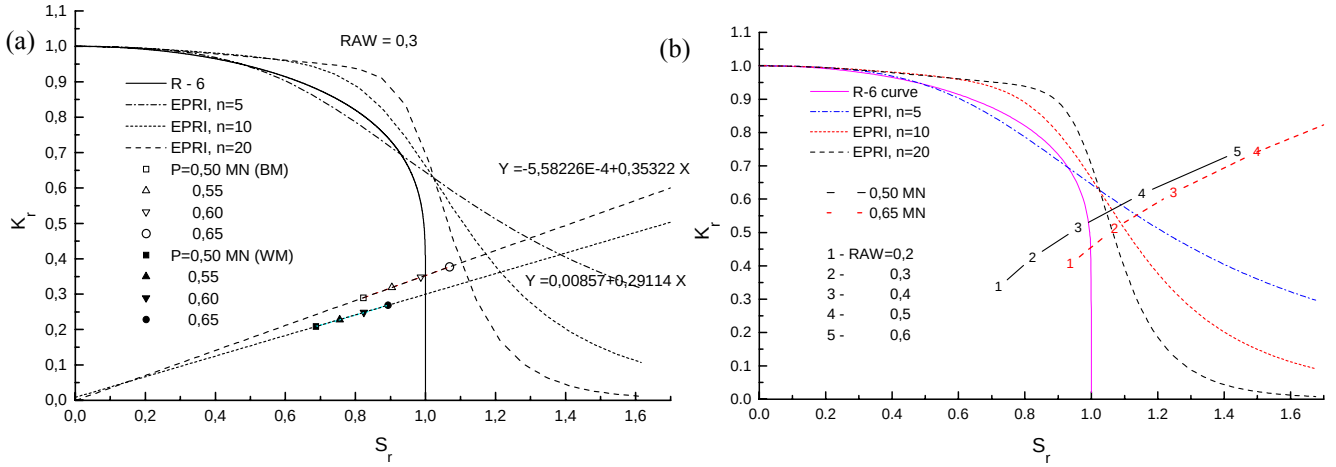

Figure 12. Plane stress failure paths for BM and WM of centre cracked specimen with load change, (a) RS = 0, (b) RS = $0.3\sigma_y$.
Slika 12. Putanja loma, ravno stanje napona, BM i WM, epruveta sa centralnom prslinom, uz promenu opterećenja, (a) RS = 0, (b) RS = $0,3\sigma_y$

CONCLUSIONS

Application of LSM in fracture mechanics enables an analysis of a part-through crack in a component represented by a plate or a shell, using first estimate of the crack for an analytical approach; if computational mechanics techniques are applied, finite element analysis should be three-dimensional. The general problem of a three-dimensional crack in a solid with given geometry is a strong interaction between the stress field disturbed by the crack and the bounding surfaces of the solid. Even in linear elasticity, an analytical treatment of the problem seems to be intractable.

REFERENCES

1. Read, D.T., McHenry, H.I., *Interim progress report: J-integral method for fitness-for-service assessment*, NBSIR 81-1648, NBS, Boulder, Colorado 1981, pp. 12-41.
2. Turner, C.E., *Methods for post-yield fracture safety assessment*, in Post-yield fracture mechanics, edited by D.G.H. Latzko, London, Applied Science Publishers, 1979, 23-210.
3. Rice, J.R., Levy, N., *The part-through surface in an elastic plate*, Journal of Applied Mechanics, March 1972, pp.185-194.
4. King, R.B., *Elastic-plastic analysis of surface flaws using a simplified line-spring model*, Engng. Fracture Mechanics Vol. 18, No 1, pp. 217-231, 1983.
5. Sedmak, S., Petrovski, B., Sedmak, A., Lukačević, Z., *The Study of crack significance in spherical storage tanks by J resistance curve*. International Conference on weld failures, London, TWI, 1988. Paper 18, pp. 18-1 / 18-10.
6. Reed, R.P., et al., *Fitness-for-service criteria for pipeline girth - weld quality*, Welding Research Council Bulletin No 296, July 1984. ISSN 0043–2326
7. Read, D.T., *Analysis of fracture mechanics and curves of allowable defect sizes for surface cracks in pipelines* (in Serbian), 3 IFMASS: Fracture mechanics of welded joints-Monograph, 324-329, Arandjelovac, June 1984.
8. Cheng, Y., et al., *Crack-opening displacement of surface cracks in pipeline steel plates*, in Fracture mechanics: fourteenth symposium, Volume II: testing and applications, ASTM special technical publication 791, Baltimore 1983, p. II-214 / II-247.
9. Sedmak, S., Adžiev, T., Sedmak, A., *Crack behaviour in HAZ of small specimens, welded panels and pressure vessels*, in 'Mechanical behaviour of materials-VI' proceedings of the sixth Int. Confer., Vol. 4, edited by M. Jono and T. Inoue, Pergamon press, Kyoto, 1991, 99-104.
10. Adžiev, T., *Residual welding stresses – the influence on behaviour of pressure cracked vessels*, 6 IFMASS: Exploitation cracks in pressure vessels and reservoirs (Vrdnik, 1991)-Monograph, edited by S. Sedmak and A. Sedmak, TMF Belgrade-European Centre for Peace and Development Beograd-Institute GOŠA Belgrade, Belgrade 1994, pp. 127-148.
11. Parks, D.M., White, C.S., *Elastic-plastic line spring finite elements for surface-cracked plates and shells*, Journal of pressure and vessel technology, November 1982, Vol. 104, pp. 287-292.
12. Erdogan, F., Aksel, B., *Line spring model and its applications to part-through crack problems in plates and shells*, Fracture mechanics: Nineteenth Symposium, ASTM STP 969, editor T.A. Cruse, American Society for Testing and Materials, Philadelphia, 1988, pp. 125-152.
13. Sedmak, S., Adžiev, T., Sedmak, A., Gočev, J., *Experimental and numerical analysis of cracked welded joints*, 11th European Conference on Fracture, ENSMA, 1996, pp.1-2.
14. Kirić, M., *The application of fitness-for-service concept to pressure vessels welded joints made of HSLA steels* (in Serbian), PhD thesis, Faculty of Mechanical Engineering, University of Belgrade, 2000, pp. 1-251.
15. Anderson, T.L., Fracture mechanics-fundamentals and applications, CRC press Inc. 1995, Texas.
16. Kirić, M., *On relations between J integral and CMOD for cylinders*, MESO-035, The 9th Conference on Mesomechanics (MESO2007), Giens (France), May 13-17, 2007, pp. 501-508.
17. Sedmak, A., The application of fracture mechanics to structures integrity (in Serbian), Monograph, edited by B. Savić, Faculty of Mechanical Engineering, University of Belgrade 2003, pp. 18-19.
18. Dowling, A.R., *The effects of defects on structure failure: a two-criteria approach*, International Journal of Pressure Vessel and Piping, 3(8), 1975, pp. 77-137.
19. Harrison, R.P., Loosemore, K., Milne, I., *Assessment of the integrity of structures containing defects*, CEGB Report No. R/H/R6, Central Electricity Generating Board, United Kingdom, 1976.
20. Kanninen, M., Popelar, C., *Advanced Fracture Mechanics*, Oxford University Press Inc., Chap. 5, 1985.

21. PD 6493 Guidance on methods for assessing the acceptability of flaws in fusion welded structures, BSI, 1991.
22. Kirić, M., Sedmak, A., Lozanović J., *An estimation of effects of heat treatment and crack length on cracked panels integrity*, First Serbian (26th YU) Congress on Theoretical and Applied Mechanics, Kopaonik, April, 10-13, 2007.
23. Adžiev, T., *A contribution to studying the influence of residual stresses on the fracture resistance of welded structures containing a crack*, (in Macedonian), Doctoral thesis, Faculty of Mechanical Engineering, University of Skopje, 1988.
24. Kumar, V., German, M.D., Shih, C.F., *An engineering approach for elastic-plastic fracture analysis*, NP-1931, Research Project 1237-1, General Electric Company, New York, Chap. 8, 1981.